CZECH TECHNICAL UNIVERSITY IN PRAGUE
FACULTY OF ELECTRICAL ENGINEERING
DEPARTMENT OF PHYSICS

Bachelor Thesis

Non-thermal electrical discharges for generation of active species

Netermální elektrické výboje pro generaci aktivních částic

Chukhlantsev Kirill

Study Program: Electrical Engineering and Computer Science

Supervisor: Prof. Ing. Stanislav Pekárek, CSc.

Prague, 2018.

BACHELOR'S THESIS ASSIGNMENT

I. Personal and study details

Student's name:	**Chukhlantsev Kirill**
Faculty / Institute:	**Faculty of Electrical Engineering**
Department / Institute:	**Department of Physics**
Study program:	**Electrical Engineering and Computer Science**

Personal ID number: **457405**

II. Bachelor's thesis details

Bachelor's thesis title in English:

Non-thermal electrical discharges for generation of active species.

Bachelor's thesis title in Czech:

Netermální elektrické výboje pro generaci aktivních částic.

Guidelines:

1. Non-thermal electrical discharges in air - fundamental physical principles.
2. Measurements of basic electrical parameters.
3. Ozone and nitrogen oxides generation - plasmachemical processes.
4. Experimental study of ozone generation for selected type of the discharge.

Bibliography / sources:

[1] A Fridman, A Chirokov and A Gutsol, 2005, Non-thermal atmospheric pressure discharges. J. Phys. D: Appl. Phys. 38 (2005) R1-R24.
[2] M. A. Malik, Nitric Oxide Production by High Voltage Electrical Discharges for Medical Uses. A Review. Plasma Chem Plasma Process 36 (2016) 737-756.
[3] S. Pekarek, Experimental Study of Nitrogen Oxides and Ozone Generation by Corona-Like Dielectric Barrier Discharge with Airflow in a Magnetic Field. Plasma Chem Plasma Process (2017). DOI 10.1007/s11090-017-9831-9.
[4] J. Mikeš, S. Pekárek, and I. Soukup, Experimental and modelling study of the effect of airflow orientation with respect to strip electrode on ozone production of surface dielectric barrier discharge. Journal of Applied Physics, 120 (2016) 173301
[5] K.H. Becker, U. Kogelschatz, K.H. Schoenbach, R.J. Barker, 2004 Non-Equilibrium Air Plasmas at Atmospheric Pressure. Institute of Physics, Series in Plasma Physics, 2005, Bristol and Philadelphia.

Name and workplace of bachelor's thesis supervisor:

prof. Ing. Stanislav Pekárek, CSc., Department of Physics, FEE

Name and workplace of second bachelor's thesis supervisor or consultant:

Date of bachelor's thesis assignment: **08.01.2018** Deadline for bachelor thesis submission: **25.05.2018**

Assignment valid until: **30.09.2019**

prof. Ing. Stanislav Pekárek, CSc.	Head of department's signature	prof. Ing. Pavel Ripka, CSc.
Supervisor's signature		Dean's signature

III. Assignment receipt

The student acknowledges that the bachelor's thesis is an individual work. The student must produce his thesis without the assistance of others, with the exception of provided consultations. Within the bachelor's thesis, the author must state the names of consultants and include a list of references.
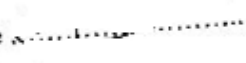
Date of assignment receipt	Student's signature

Declaration

I hereby declare that this thesis is the result of my own work and all the sources I used are in the list of references, in accordance with the Methodological Instructions of Ethical Principle in the Preparation of University Thesis.

K.Chukhlantsev, Signature ....

In Prague, 20.04.2018

Acknowledgment

Abstract

This thesis is dedicated to the generation of active species, such as ozone (O_3) and various types of nitric oxides (NO_x), with non-thermal electrical discharges. Theory of dielectric barrier discharges, positive and negative corona discharges together with the typical electrode systems are described. The thesis includes brief economical evaluation of modern technologies of O_3 and NO_x production and historical overview of this active species generation. Applications of O_3 and NO_x are discussed.

Key Words

Ozone, nitrogen oxides, non-thermal electrical discharges, dielectric barrier discharge, corona discharge.

Abstrakt

Tato práce je věnována tvorbě aktivních částic, jako je ozon (O_3) a různé typy oxidů dusíku (NO_x) netermálními elektrickými výboji. Je popsána teorie dielektrického bariérového výboje, kladné i záporné korony společně s charakteristickými elektrodovými systémy těchto výbojů. Práce zahrnuje stručné ekonomické zhodnocení moderních technologií generace O_3 a NO_x a historický přehled generace těchto aktivních částic. V práci je také diskutováno použití ozonu a oxidu dusíku v různých aplikacích.

Klíčový slova

Ozon, oxidy dusíku, netermální elektrické výboje, dielektrický bariérový výboj, korónový výboj.

Table of contents

List of used abbreviations

DBD	...	Dielectric Barrier Discharge
SDBD	...	Surface Dielectric Barrier Discharge
UV	...	Ultra Violet
IR	...	Infrared
DMM	...	Digital Multimeter
RMS	...	Root Mean Square
PC	...	Personal Computer
WPA	...	Wideband Power Amplifier

1. Introduction

The problem of generation of active species starts its history in the 18th century. In the 1785 year scientist M. Van Marum discovered a strange odor in close vicinity of an electrostatic machine, but the source was discovered more, than 50 years later. In 1839 prof. Schonbein established that this smell was caused by a new compound that he coined with the word „Ozone". It took 25 years to discover that ozone was made up of 3 atoms of oxygen (O_3). The first ozone generator, working on DBD (dielectric barrier discharges) was invented by German electrical engineer Werner von Siemens in the 1857 year. Ozone, being an extremely effective oxidant, made the water absolutely sterile after treatment. This technology helped to take control on the Cholera bacteria that was transferred mainly with contaminated water in the 19th century, and purify the water from other biologically dangerous bacteria (such as typhus and coli bacteria).

From that time ozone and various forms of nitric oxide found application in medicine, agriculture, sterilization of biologically contaminated environments and water purification. Nowadays ozone treatment partly substituted the purification of water with chlorine that was considered as unsafe for the environment.

Devices, generating ozone, are functioning on non-thermal electrical discharges, such as positive and negative corona and dielectric barrier discharge, because ozone decays fast at elevated temperature. With the increase of temperature the NO_x molecules, mostly NO and NO_2 would be generated.

Nowadays continuous improvement of technologies leads to increase of quality of production, reliability and lifetime of devices. The decrease in cost of the generated species plays an important role in utilization them in production.

2. Non-thermal electrical discharges in air.

In general, an electrical discharge is considered a non-thermal in case that the plasma, produced with the discharge is not in a thermodynamic equilibrium (for example the temperature of ions and electrons is different) that is why non-thermal plasmas are sometimes called non-equilibrium. Non-thermal discharges have several advantages in comparison with thermal ones, the most important is the energy efficiency in plasma-chemical processes. Nowadays a vast variety of non-thermal discharges is known and studied, among them are spark discharges, gliding ark discharges, DBD, surface discharges, positive and negative corona, pulsed corona discharges, etc. In this project, 3 types of discharges (DBD, positive and negative corona) are discussed, due to their properties being the most suitable in ozone and nitric oxides generation (mostly due to a low temperature of working gas and high number of application in modern science). The experimental part of the project is focused on DBD, operating in normal air and atmospheric pressure conditions. The condition of normal air utilization is crucial for economic efficiency and application simplicity of the devices, build up on the studied discharges.

2.1. Townsend breakdown.

The discharge itself is associated with the breakdown phenomenon in gases with further formation of a conductive channel. Most of the discharges usually start with electron avalanche. The avalanche starts from a released electron (for example as a result of cosmic rays' impact) in close vicinity of a cathode that is been accelerated with presented electric field to the direction of the anode. Moving through the gap d (see Fig. 1) between cathode and anode in a gas that could be ionized (for example air), electron collides with other molecules, staring the primary ionization. This phenomenon is known as Townsend breakdown. The schematic diagram of the electron avalanche is presented in Fig. 1.
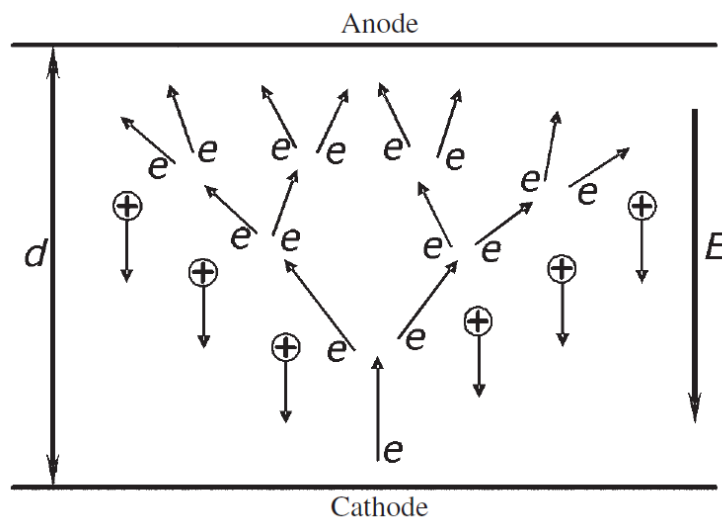

Figure 1: Illustration of Townsend breakdown [1].

The positive ions generated due to the collision with electrons move under the electric field to the cathode. Upon a collision with the cathode an ion might release an electron, this process is known as secondary electron emission. The probability of an electron to be released upon a collision on the cathode is dependent on the material, the cathode is made of, and refers to the secondary emission coefficient γ that is also called "third Townsend coefficient". Typical values of the γ coefficient are 0.01-0.1 [1]. An electron avalanche develops both in time and in space, due to electron multiplication during their drift from cathode to anode that is why it is convenient to describe the ionization in avalanche not with ionization rate coefficient, but with Townsend ionization coefficient α that is sometimes called "first Townsend coefficient". This coefficient expresses the electron production per unit of length along the electric field [1]:

$$\frac{dn_e}{dx} = \alpha n_e \tag{1}$$

The current in the gap becomes self-sustained if the breakdown condition is valid [1]:

$$\alpha d = \ln(\frac{1}{\gamma} + 1) \tag{2}$$

i.e. for a breakdown to happen, the generated ions must release at least 1 electron from the cathode to begin a new avalanche.

2.2. Positive streamer.

When the internal electric field of an electron avalanche becomes comparable with the external applied electric field the avalanche-to-streamer transition takes place. The condition for this transition is known as "Meek's breakdown condition" and is referred to the amplification parameter: $\alpha d \geq 20$ [1]. A streamer is a channel of weakly ionized plasma. In small discharge gaps, the transition takes place only when the avalanche reaches the anode. The streamer starts near anode and propagates towards the cathode that is why such a streamer is called cathode-directed, or positive. After the streamer connects the two electrodes with a conductive plasma channel the current is significantly increased to form a spark.

2.3. Dielectric Barrier Discharges.

At the moment of discovery in XIX century by W.V. Siemens the phenomenon was called a "silent discharge", because of the absence of any noise, following the process. Later on, the name was modified to the DBD, since the key role in the discharge is played by the dielectric layer. DBD can be obtained in an electrode arrangement, where the gap d (Fig. 1) is filled with a dielectric material (ceramic material or glass could be used, having high dielectric strength and relatively low losses). The dielectric prevents the spark

formation and the DC current to be conducted through the gap. Among benefits of DBD utilization is highly non-equilibrium conditions with a non-complex AC power source setup.

The typical arrangement for an electrode system for DBD generation are: planar or cylindrical (using the coaxial plates), illustrated in Fig. 2. The gap clearance may vary from 100 μm to 2-3 centimeters, depending on the actual application of the device.
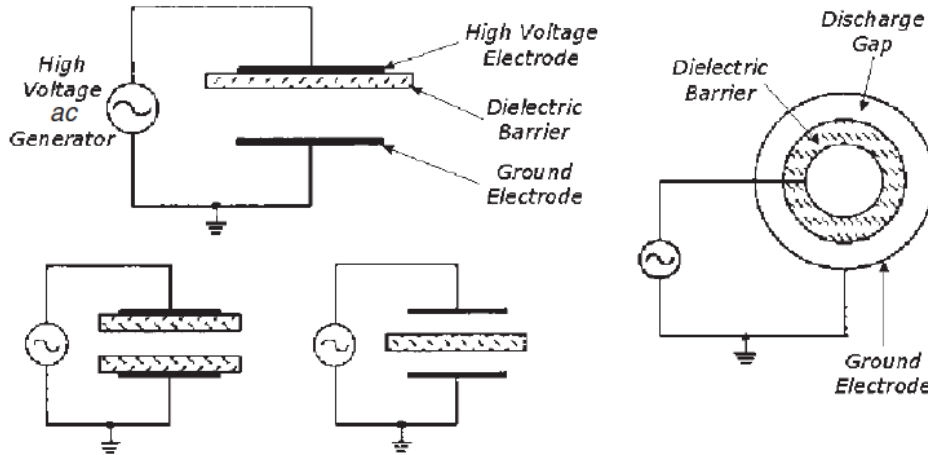

Fig. 2: Common DBD configurations [1]

Gap clearance is an object of many studies, the experimental result of the gap variation from 0.5 mm to 1.5 mm as a diagram of visible optical emission intensity for 2 different frequencies – 500 Hz and 600 Hz is illustrated in Fig. 3. More information about the experimental study could be found at [6].
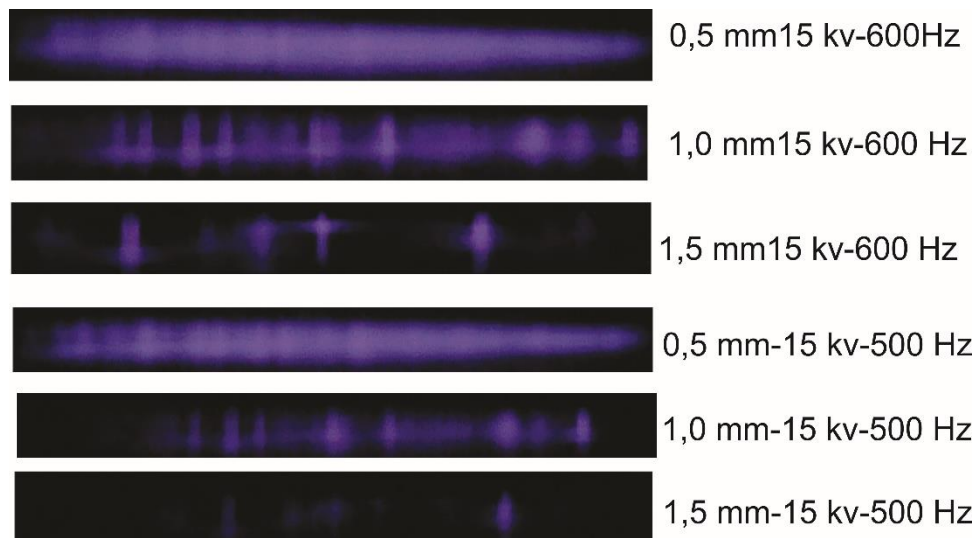

Fig 3: Visible Optical emission intensity resulting from atmospheric DBD at 600 and 500 Hz frequencies. [6]

Usually, a DBD is formed up of a large number of microdischarges and thus is non-uniform. The first study of the nature of the DBD referring the process to a large number of tiny breakdown channels (microdischarges) was made by Klemenc in 1937 [1]. The phenomenon of a microdischarge is associated with the formation of streamers and further plasma channel degradation. The process of the discharge begins with an initial electron, moving from the cathode to anode and ionizing the media. If the electric field is strong enough the electron avalanche starts, then if the avalanche is sufficiently large (the Meek's breakdown condition is valid) a cathode-directed streamer is initiated.

Moving alone the gap a streamer forms a channel of plasma that is conductive. Electrons will flow through the channel and would accumulate on the anode, causing the high current. After the electrons accumulate on the dielectric surface, the local electric field collapse and the conductive channel is terminated. This process, starting from the electron avalanche till the channel termination is called the "microdischarge".

However, the behavior of electrons and ions is different: being light and fast electrons dissipate from the gap at a time around 40 ns while heavy ions stay in the gap for a time up to microsecond. Usual operation frequency for a driving AC power source in DBD utilization is from 500 Hz to 500 kHz. In case that we assume a typical frequency of operation to be 20 kHz, then the polarity of the voltage is reversed every 25 µs. In the study of DBD, the change of polarity is a crucial point, since charge, accumulated in the close vicinity of anode dielectric barrier prevents new streamers and electron avalanches until the change of polarity.

If the conductive channel would terminate without any circumstances for the whole physical system the breakdowns should be distributed more uniformly. There exists another physical phenomenon, associated with microdischarge that explains high non-uniformity of the breakdown distribution (see Fig. 3).

This phenomenon is known as "memory effect". When the channel is terminated there is no more plasma present at the microdischarge gap, however high level of excitation and vibration in the gap d (see Fig. 1) make it possible to separate this region from the other dielectric. This region is called the microdischarge remnant. Heavy and slowly drifting ions are present in the remnant. Those ions move towards the electrodes causing a low ion current. This remnant current will support the further formation of the microdischarges in the same region of the dielectric that is why it is possible to observe the "filaments", groups of microdischarges in the same region, when the polarity is changed. The short duration of a microdischarge results in low overheating of the channel and the generated plasma remains cold, or non-thermal, making DBD an attractive method of generation of active species that require a low temperature of working media. Typical characteristics of a microdischarge are presented in the Tab. 1 [1].

Lifetime	1–20 ns	Filament radius	50–100 μm
Peak current	0.1 A	Overheating	5 K
Total transported charge	0.1–1 nC	Gas temperature	Close to average, about 300 K

Tab 1: Typical parameters of a microdischarge.

2.4. Corona Discharges.

A corona discharge is a physical phenomenon that can exist in the close vicinity of a conductor with a small radius of curvature, i.e. where the non-uniform electric field is present. Usually, corona discharge can be observed on the top of trees or at masts of ships (the phenomenon is known as "Saint Elmo's fire") in nature, near the high voltage transmission lines or around lightning protection rods as weak luminous glow. It is important to state that in power engineering and high voltage transmission line design a corona discharge is an unwanted side effect that causes losses in power transmission and decreases the efficiency of transmission. If the region of a corona discharge is humid enough the ozone, generated by the discharge, may form new compounds, such as nitric acid. These compounds are corrosive to metal parts of construction, thus decreasing the lifetime of the equipment and are toxic to people. The reason for corona discharge to exist is poorly limited electric field that let a conductive region to form around sharp shape of a conductor but is not strong enough for arc breakdowns to other conductive objects. If the electric field is elevated to even higher values the corona to spark transition occurs, causing the breakdown of the gap to the electrode. Spontaneous corona, being an unwanted effect, is often tried to be liquidated by engineers, however, a controlled corona discharge is a promising technology in active species generation field.

The mechanism of sustaining the continuous ionization depends on the polarity of the electrode, where the discharge is located. That is why two types of corona discharge are distinguished: positive and negative corona.

2.4.1. Positive Corona Discharges.

If the high electric field is present in the vicinity of the anode such corona is called a positive one. In this case, electrons are attracted to the electrode, and ions are repelled. The ionization is related to the cathode-directed streamers. The ignition criteria are described using the condition of such streamer formation. If considered high non-uniformity of the discharge, a generalized Meek's breakdown condition would be a good approximation [1]:

$$\int_0^{x_{max}} [\alpha(x) - \beta(x)]dx \approx 18 - 20 \tag{3}$$

Where $\alpha(x)$ is the first Townsend coefficient, $\beta(x)$ is the second Townsend coefficient, describing ionization and electron attachment respectively, and x_{max} stands for the distance from the electrode, where the electric field is low enough for the following condition to be valid:

$$\alpha(x_{max}) = \beta(x_{max}) \tag{4}$$

The condition (4) means, in another word that no further electron multiplication takes place. It is important to state that condition (4) also determines active corona zone that is responsible for corona glow, so the critical distance from the electrode might be also taken as a visible zone of corona (however, corona radiates also in invisible spectrum, this can be proved easily using a photo camera that is not equipped with a UV and IR filter) (see Fig. 4). On the contrary to the uniform glow on negative corona, in the positive corona, the individual high luminous streamers could be observed.
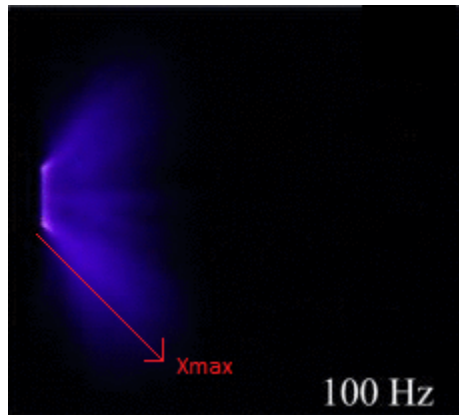

**Fig. 4:** Active (visible) corona zone at 100 Hz frequency [7].

2.4.2. Negative Corona Discharges.

In case the high electric field is concentrated near cathode this corona is called negative. The current from the cathode into the plasma is continuous due to secondary emission from the cathode. This is the crucial difference between the physical phenomenon of a positive and negative corona. Far from the electrode under the conditions of the weaker electric field, when the energy is not enough for an electron avalanche, the electrons start to attach to neutral molecules, creating negative ions that are responsible for current in an outer zone of a discharge ($>x_{max}$) (see (3)). As stated above, the ignition of a negative corona involves the same mechanisms as Townsend breakdown, and to estimate it mathematically the possibility of electron attachment is need to be considered [1]:

$$\int_0^{x_{max}} [\alpha(x) - \beta(x)] dx = \ln(1 + \frac{1}{\gamma}) \tag{5}$$

This equation is similar to (3), γ stands for the third Townsend coefficient, describing the secondary electron emission from the cathode. It is important to state that if the working media is not an electronegative gas (second Townsend coefficient is equal to zero), i.e. no electron attachment is possible, the integration in (5) is formally not limited, but the condition of taking the limit to x_{max} as an effective distance is rational due to exponential decrease of $\alpha(x)$. Critical values of electric field for positive and negative corona ignition are close, even though two very different mechanism of breakdown are related to those phenomena.

In terms of industrial utilization, the ozone and nitric oxide formation are restricted to the thin active corona region of high ionization that is why a separately controlled corona discharge is rarely considered as an industrial method of active species production [5]. The active volume of the corona discharge (see Fig. 4) is strictly dependent on the value of the electric field that corresponds to the breakdown value on the boundary of the active volume.
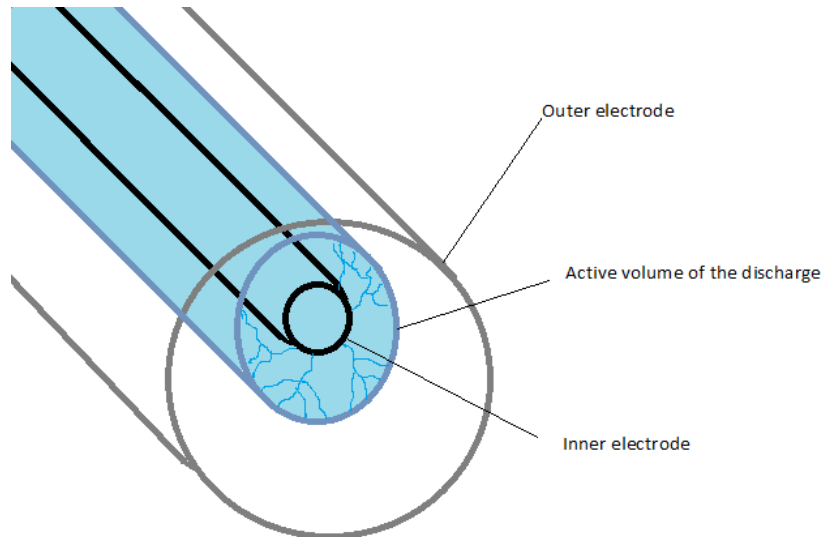
Fig. 5: Active volume of corona in case of coaxial (cylindrical) electrode system.

3. Measurement of basic electric parameters.

There exist a large number of parameters to be measured in a study of an electrical discharge, but the fundamental quantities are voltage and current. The measurement of voltage and current is always dependent on individual features of an experiment and equipment setup that is important to consider during the further calculation of electric power, released in the discharge. A vast variety of sensors for measurement of electrical parameters is available on the market. The uncertainty and precision of the utilized sensor is not only the matter of price but also the technology, the device is built on.

For each measurement, the Type A (based on statistical analyses, associated with the estimated standard deviation of the mean) and Type B (associated with the method of measurement and uncertainty of measuring devices) uncertainty are often calculated. In case of power calculation from voltage and current multiplication, the uncertainty of combined measurement is to be derived. It is essential to understand the principles of used sensors operation to analyze the results of the experiment correct.

3.1. Measurement of voltage.

There exist a lot of devices to measure voltage, depending on required range, a variation of value and setup of experimental apparatus. The direct measurement of voltage is possible up to 200 kV, which is more, then enough for applications in electrical discharges. A high voltage probe, being relatively simple and robust sensor, might be a good choice for the required application.

A high voltage probe is a device that reduces the input voltage to a level that would be safe for a regular DMM. The probe, intended for usage below 100 kV, encapsulated inside a high accurate resistive voltage divider. To achieve high linearity and accuracy of the device, the resistors with extremely low voltage coefficient must be used. A typical electric circuit for a high voltage probe connection is illustrated in Fig. 6.
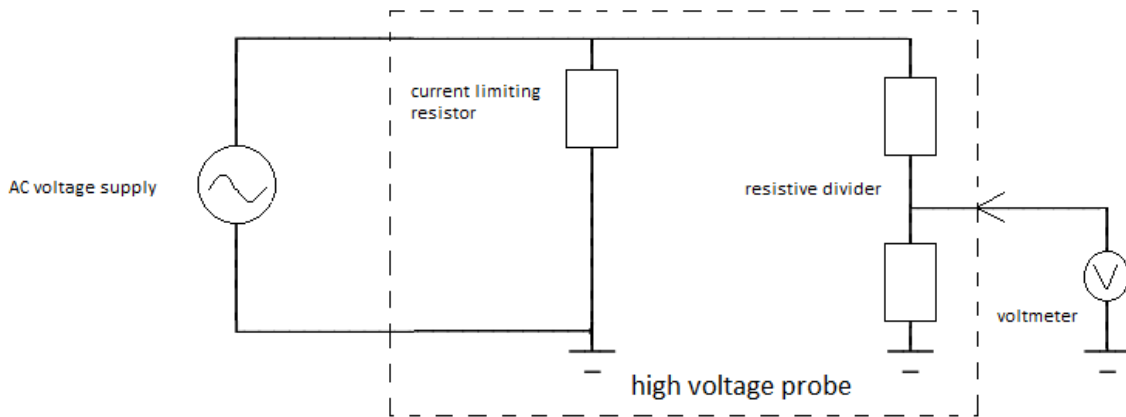

Fig. 6: Typical electric circuit for high voltage probe connection.

A combination of probe and measuring instrument must have a high input impedance (especially the reactive component) in order not to affect the measured voltage. A DMMs' input impedance, however, might alter the dividers ratio decreasing the accuracy of the device.

A probe should have as low input capacitance as possible to decrease the parasitic effects. Parasitic capacitance, combined with probe's impedance, forms an RC circuit that will also disturb the measurement.

To eliminate these effects probes are usually equipped with additional components that improve the frequency response and allow calibration for different DMM loads.

A high voltage probe that is utilized in the experiment, described in this thesis, is "Pintek HVP-28 HF". The probe has the following characteristics:

- Maximum input DC voltage – 28 kV
- Maximum input AC voltage – 20 kV RMS
- Bandwidth – up to 200 MHz
- Input impedance – 500 MΩ
- Input capacitance – 1.7 pF

The device average cost is around 450 USD (approximately 9.500 CZK). The device is illustrated in Fig. 7.

Fig. 7: High voltage probe.

3.2. Measurement of current.

Another fundamental electrical parameter to be measured is current in the discharge. In case of DBD study, the AC current is to be measured. The measuring tool should be chosen according to the specifications of the experiment.

The DBD often results in high current peaks due to streamers formation and general non-uniformity. Regular measuring apparatus might be simply not fast enough in terms of response to rapid current changes.

3.2.1 Rogowski coil.

One of the possible solutions is the utilization of Rogowski Coil. Named after the German physicist Walter Rogowski, the Rogowski Coil is a current transformer, that consists of the evenly wound coil on a non-magnetic former with the constant cross-sectional area. The winding wire is returned to the starting point through the central axis of the former. It is important to have a constant distance between the turn of the wire to decrease the parasitic capacitance. Then the 2 ends of the wire are usually connected to a cable. The device has no metal core. The coil is then wrapped around a conductor in which the current is to be measured.

In a coil the voltage is proportional to the derivative of the magnetic flux with respect to time [11]:

$$v(t) = \frac{AN\mu_0}{l} * \frac{di(t)}{dt} \tag{6}$$

In the equation (6) A is the area of one of the small loops, N is the number of turns of the coil, l is the length of the wiring, μ_0 is the magnetic constant $(4\pi*10^{-7}\frac{V*s}{A*m})$.

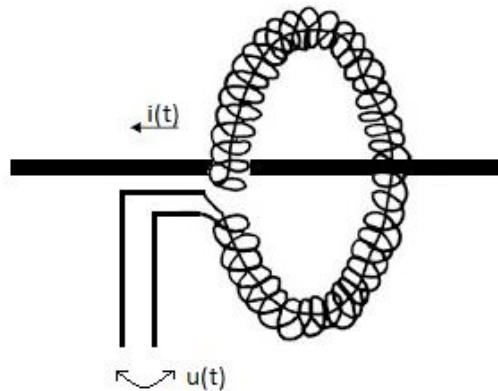The typical arrangement of the coil is shown in Fig 8:

Fig. 8: Rogowski Coil, wrapped around conductor.

Since the Rogowski Coil output is voltage, to obtain the quantity proportional to the current in conductor an integrator should be used in electric circuit. It might be a simple RC low pass filter with an operational amplifier. Usually, a lossy integrator is used to reduce the effect of offset voltages. The typical electric circuit is illustrated in Fig 9.

Among other benefits of the instrument there are:

- Very low cost
- Easy operation
- Higher accuracy, then in common current transformers
- High linearity due to the absence of magnetic core saturation
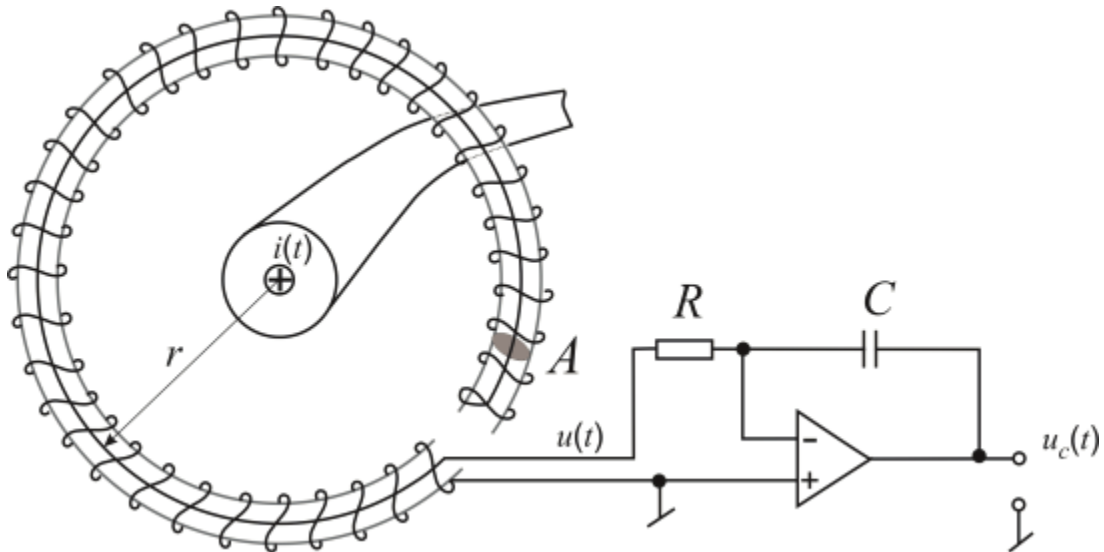
Fig. 9: Typical electric circuit for Rogowski Coil (source: www.researchgate.net)

Rogowski Coil is unresponsive to DC current that makes the device capable to measure very low current with high DC component.

The current measuring device that was utilized in the experiment, described in this thesis is called "Pearson Current Monitor 2877". This sensor incapsulates the Rogowski Coil. The sensor is illustrated in Fig. 10.

The device has the following specifications:

- Maximum peak current – 100 A
- Sensitivity 1 Volt/Ampere +1/-0%
- Maximum RMS current – 2.5 A
- Output resistance – 50 Ω
- Frequency range – 300 Hz – 200 MHz
- Operating temperature – 0 to 65 ºC
- Usable rise time 2ns

Fig. 10: Pearson Current Monitor 2877

The average cost of the device is 335 USD (approximately 6900 CZK). The capability of the device to sense high current pulses makes it a good choice of current sensor in the study of DBD.

3.3. Calculation of power.

The calculation of average power is an essential step in analyses of active species generation. The correct supply of power to plasma generators is required to keep the high efficiency of generation and lifetime of the equipment. The power is an amount of work done per unit of time. In the simplest case, the instantaneous electrical power is known to be the product of voltage and current. For the calculation of power of DBD, there exists two applicable methods are described.

3.3.1. Calculation from instantaneous voltage and current.

In study of DBD both voltage and current are functions of time, and the calculation of average power is done with following formula:

$$\bar{P} = \frac{1}{T} \int_0^T v(t) * i(t) dt \qquad (7)$$

In equation (7) T is the period, for which the average power is to be calculated, v(t) and i(t) are voltage and current function, dependent on time. Another possible approach to average power calculation is to find it from the total energy, dissipated in the discharges. Power is known to be the derivative of energy with respect to time. From (9) it is seen that the integral is, in fact, equal to the whole energy, dissipated in the

discharge. Energy, dissipated in the discharge is equal to the area of the Lissajous figure, associated to the studied discharge.

3.3.2 Calculation from Lissajous figures.

Lissajous figures (or Lissajous curves) are graphs with closed trajectories of systems of equations that describe complex harmonic motion. Named after French physicist Jules Antoine Lissajous, those graphs find applications in the analysis of phase relationship of two signals, memristor testing etc. The Lissajous figure is drawn by a point that simultaneously performs harmonic motion in two perpendicular axes. The shape of the figure depends on the relation between amplitude, frequency and phase shift of the two input signals. The two signals are defined with the system of equations:

$$\begin{cases} x(t) = A sin(\omega_1 t + \varphi) \\ y(t) = B sin(\omega_2 t) \end{cases} \tag{8}$$

In equation (8) A and B are amplitudes, ω_1 and ω_2 – frequencies of the two signals and φ – the phase shift between them. In case ω_1 and ω_2 are φ is equal to zero the curve turns into a straight line. This effect takes place, because a point is moving along the y and x axis with same frequency and phase, so being added together they form a curve, corresponding to equation $x = y$. If A and B are equal and $\varphi = \frac{\pi}{2}$, the graph is a circle. To observe this effect on an oscilloscope it is enough to choose the X-Y mode and feed two signals with corresponding properties. To see the actual movement of the point, constituting the Lissajous figure, it is required to set the frequency of the signal low enough.

In case of an experiment where both the voltage and current are harmonic functions of time the Lissajous figures might be applied as a method of analyses. Lissajous figures as a charge vs voltage characteristic provide important information about nature and properties of the DBD.

The average power could be calculated with the following formulae:

$$\bar{P} = f * E \tag{9}$$

In equation (9) f is the frequency of the driving voltage and E is the energy, calculated as an area of the Lissajous figure, associated to the investigated discharge.

4. Plasma-chemical processes.

Plasma-chemistry deals with high ionization of working gas, in this way, making it possible to generate active species with high efficiency and high purity. Besides the efficiency, utilization of plasma technologies in chemistry let the increase of automation of the processes, which leads to the decrease of price of produced species.
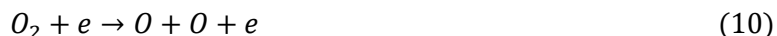
4.1. Nitrogen Oxide Processes.

NO stands for nitric oxide sometimes called nitrogen monoxide. It was called the "nitrous air" at the time of discovery. In conditions of room temperature and atmospheric pressure, it is a colorless gas. Nitric oxide is difficult to liquify, in liquid and solid state it has light-blue color. NO is one of the oxides that includes nitrous oxide N_2O, dinitrogen oxide N_2O_2, nitrogen dioxide NO_2, dinitrogen trioxide N_2O_3, dinitrogen tetraoxide N_2O_4 and dinitrogen pentaoxide N_2O_5. Nitric oxide is an important biochemical element, broadly utilized in the synthesis of fertilizers, explosives, nitric acid and plasma medicine. Nitric oxide is a universal antimicrobial factor that kills parasites, bacteria, and fungi, without killing human cells. The physicochemical properties of nitric oxide are shown in Tab. 2:
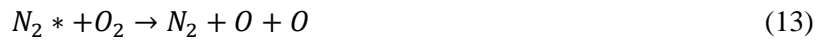
Chemical formula	NO
Boiling point	−152 °C
Melting point	−164 °C
Molar mass	30.01 g/mol
Ionization energy	9.27 eV
Solutability in water	0.01 g/100 ml

Tab 2: Basic properties of nitric oxide.

Nitric oxide is responsible for the phenomenon of acid rains, it is formed in lightning discharges in nature. In case of non-thermal electrical discharges and regular air utilization the following reactions are responsible for the NO formation [2]:

The electron initiated reactions, bringing the N and O molecules into the excited state:

$$O_2 + e \rightarrow O + O + e \tag{10}$$
$$O_2 + e \rightarrow O + O * + e \tag{11}$$

$$N_2 + e \rightarrow N_2 * + e \tag{12}$$
$$N_2 * + O_2 \rightarrow N_2 + O + O \tag{13}$$

In the previous equations * represent the excited state of the molecule. Then, those active species react with each other, forming the nitric oxide and other active species:

$$N_2 * + O \rightarrow NO + N * \tag{14}$$
$$N * + O_2 \rightarrow NO + O \tag{15}$$
$$N_2 * + O_2 * \rightarrow 2NO \tag{16}$$
$$N_2 * + O_2 \rightarrow N_2 + O + O \tag{17}$$

Some of the nitric oxide is also generated by the reaction of radicals:

$$N + O \rightarrow NO \tag{18}$$

In case of low-temperature discharges, there would be also a concentration of ozone present in the working gas. Ozone, being a high oxidizing agent would lead to NO oxidation to NO_2, NO_3, and N_2O_5 with the following reactions:

$$O_3 + NO \rightarrow NO_2 + O_2 \tag{19}$$
$$O_3 + NO_2 \rightarrow NO_3 + O_2 \tag{20}$$
$$NO_3 + NO_2 \rightarrow N_2O_5 \tag{21}$$
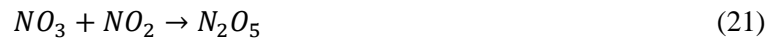
The Fig.12 illustrates the full process of formation and conversion of various types of nitric oxides and ozone in non-thermal discharge applications [2].
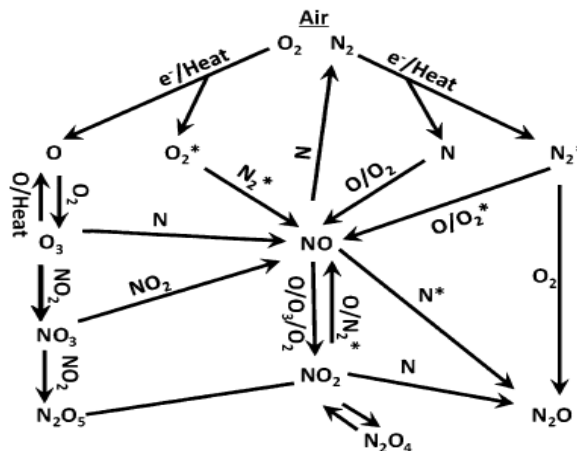
Fig. 11: Illustration of the reaction mechanisms, involved in the formation and removal of nitrogen oxides and ozone.

Nitric oxide finds applications in medicine, especially in oxide-inhalation therapy. Such a treatment could be used in case of pulmonary hypertension and acute respiratory failure. This technology, in case of appropriate dose level of NO, is approved even for infants (by US FDA) [2]. In case of therapy for children and adults, the NO inhalation may prevent the brain damage, caused by cardiac arrest anemia. An important application involves treatment of the chronic wound, reducing the level of bacterial load contamination and fasten the healing.

However, nowadays this therapy is expensive – "To date, the only consistent delivery of gNO is through direct application of gNO from a tank delivered via tube and topical applicator. Unfortunately, this renders patients non-ambulatory and bears significant cost", "This approval delivery modality for NO is expensive. The cost of the NO is ~6USD/l, bringing the cost of treating a newborn with this gas to almost $12.000, with a minimum charge of $3000 to open the tank of gas for any application" [2].

The goal of research in this field is to decrease the prime cost of production and make the application easier. The plasma devices, operating on non-thermal electrical discharges is a promising technology to make the NO treatment more affordable for people.

4.2. Ozone Processes.

Another important active molecule that is being generated in non-thermal discharges is ozone. Ozone consists of 3 atoms of oxygen and has chemical formula O_3. It is an extremely effective oxidant, comparable in oxidizing power only with radicals like OH and O or fluorine. Under normal conditions, it is an almost colorless gas, in liquid form it has indigo blue color, in solid form the color is changed to deep blue-violet. The physicochemical properties of ozone are listed in Tab. 3.

Chemical formula	O_3
Boiling point	−112 °C
Melting point	−197 °C
Molar mass	47.99 g/mol
Ionization energy	12.52 eV
Solutability in water	0.106 g/100 ml

Tab 3: Basic properties of ozone.

In liquid form the ozone is highly explosive that is why it is used only in the diluted form in gases or water stream. Ozone is a toxic gas and it is dangerous for human in concentration more than 0.15 ppm, however ozone half-period is relatively low (from second to several minutes, depending on ambient conditions), and it decomposes into oxygen that is safe for human and environment. Ozone exhibits high light absorption at wavelength 245 nm, the ozone in atmosphere of Earth absorbs most of the UV radiation from Sun, protecting the live species.

One of the most important applications of ozone nowadays is water purification and decontamination. Due to high oxidizing power ozone is never transported, but generated on a site at a rate, required in utilization in processes [5]. The largest amount of ozone for practical applications in generated with non-thermal electrical discharges. The first ozone-generating device was built by German scientist Ernst Werner Siemens in 1857. The discharges were generated in coaxial electrode system with a supply of oxygen via a tube from a glass tank. The device is illustrated in Fig. 12.
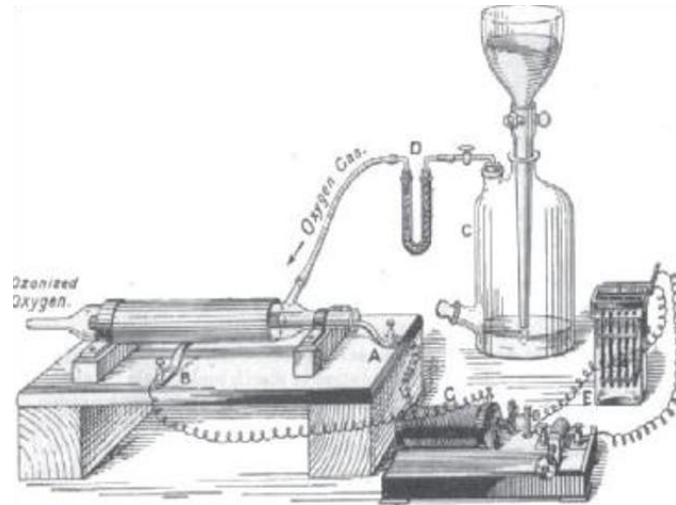

**Fig. 12:** Ozone generating device, build by W.V.Siemens (1857) [9].

Ozone is generated in discharges, where the electron energy is high enough to dissociate the O_2 molecules and the temperature of working media is kept low enough for molecules of O_3 to survive. In the discharge the electrons with high energy (the required energy is from 6 up to 8.5 eV [5]) dissolve the molecules on nitrogen and oxygen in the following reaction [5]:

$$O_2 + e \rightarrow O + O + e \tag{22}$$
$$N_2 + e \rightarrow N + N + e \tag{23}$$

In the previous equation, *e* stands for free electron. The required energy for this dissolution is supplied with electrical discharges in working gas. Then, in case of atmospheric pressure, the ozone is formed with the following reactions [5]:

$$O + O_2 + O_2 \rightarrow O_3 + O_2 \qquad (24)$$

$$O + O_2 + N_2 \rightarrow O_3 + N_2 \qquad (25)$$
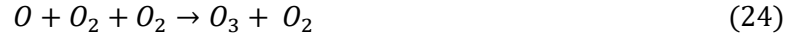
The proper power supply has a large impact on ozone generation efficiency because it is possible to optimize the generation process. The width of the discharge gap is an important parameter that influences the efficiency of ozone formation. In [10] the ozone generation from two hollow needles to plate electrical discharges was studied. The results show that in case of the electrode arrangement, described in [10], the largest concentration of ozone was achieved with 4.85 mm discharge gap. The dependence of O_3 concentration on current for different inter-electrode distance is shown in Fig. 13 [10]:
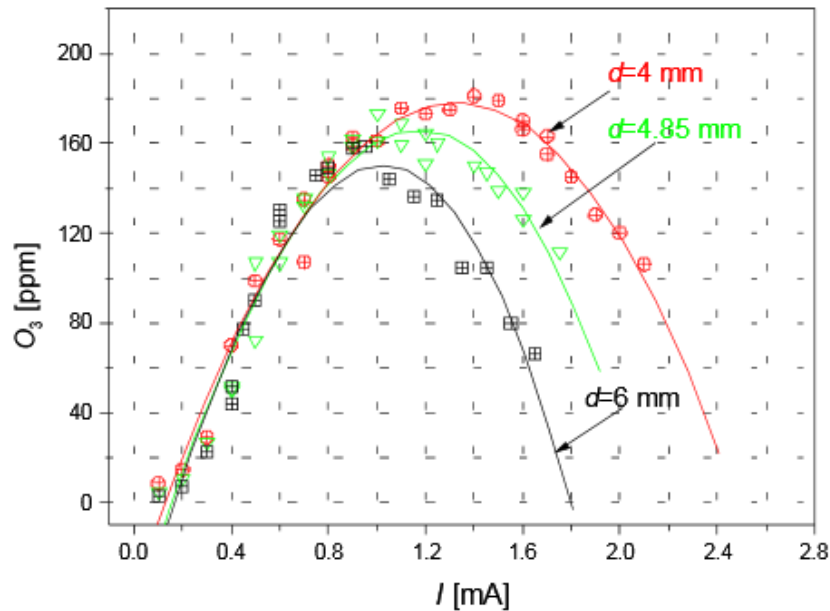
Fig. 13: Concentration of ozone versus discharge current for discharges with simultaneous both needles operation, for different distances *d* between the tips of the needles and plate electrode.

With the increase of temperature, the concentration of generated ozone decreases and nitrogen oxide molecules become predominant. This is why the atmospheric pressure and low gas temperature are the crucial conditions in ozone generation. There also exists an effect of „discharge poisoning" that is referred to the presence of NO and NO_2 molecules in working gas.

The modern industrial ozone generators (see Fig. 14 [5]) may operate on prepared gas (oxygen) or on ambient air. Among benefits of oxygen, utilization is higher efficiency and less energy consumption per 1

kg of ozone, but it also requires a prepared gas of high purity (NO_x, H_2, and hydrocarbons significantly decrease the ozone formation).

In industry, the energy that is needed to produce 1 kg of ozone varies from 7.5 to 10 kWh in case of oxygen utilization and from 15 to 20 kWh in case of regular air [5]. The current price of ozone is around 2 USD/kg. A better understanding of properties of microdischarges and research in semiconductor physics results in improvement of generating devices, their reliability, and efficiency.

An important factor is the size and weight of the devices, having an impact on maintenance and mobility of the apparatus. The study of dielectric materials will also improve the generation efficiency and increase the stability.
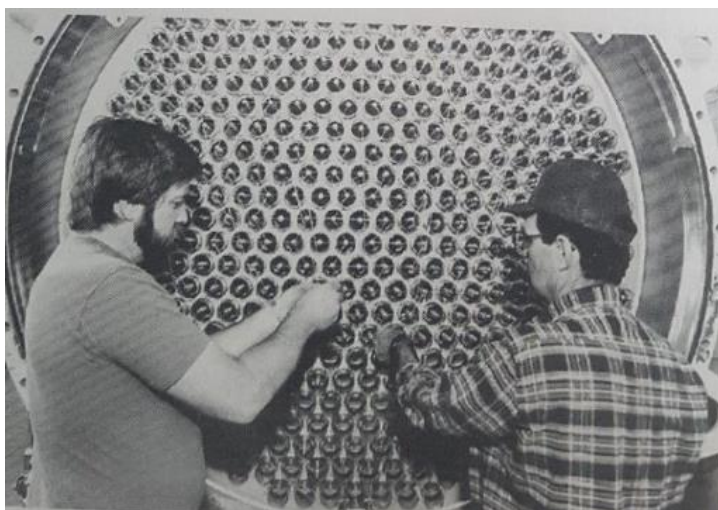

Fig. 14: Large ozone generator at the Los Angeles Aqueduct Filtration Plant.

The future research in the field of non-thermal electrical discharges will lead to a decrease in cost of the generated active species, making it more affordable.

5. Experimental study of ozone generation by DBD.

The experimental arrangement, utilized in our experiment, consisted of air tank with compressor, mass flow controller, system of pipes for air supply (part of the pipe was filled with humidity absorbing material to prevent the H_2O molecules from reaching the discharge chamber), discharge chamber with one electrode, in form of 9 interconnected parallel strips on one side of the dielectric plate and a square electrode on the other side and the cooling system to control the temperature in the discharge chamber.

In the experiment the strips electrode was connected to the wideband power amplifier, amplifying the input waveform from waveform generator and the square electrode was grounded. The diagram for the whole experimental arrangement is presented in Fig. 15:
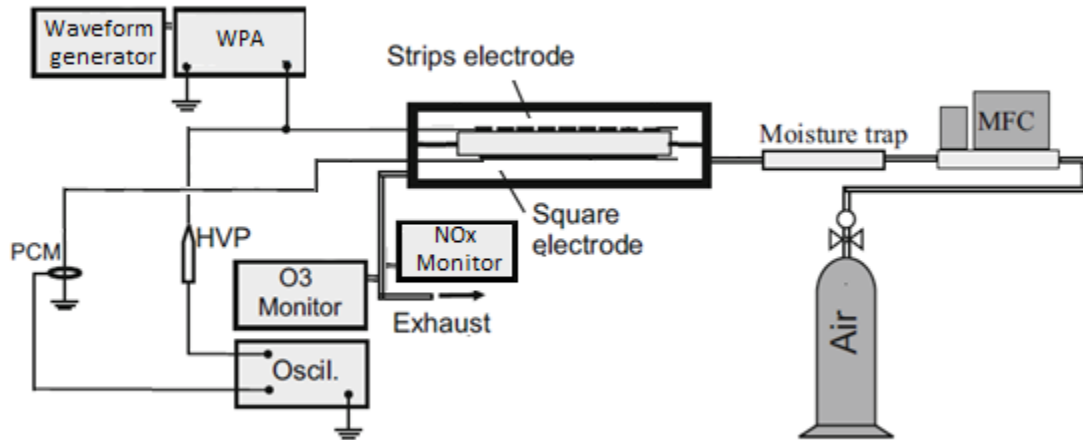
Fig. 15: The experimental arrangement.

It is seen from Fig. 16 that at high enough applied voltage (approximately >2.8 kV) it is possible to observe the glow of the electrical discharge, the peak discharge current was 0.015 A.
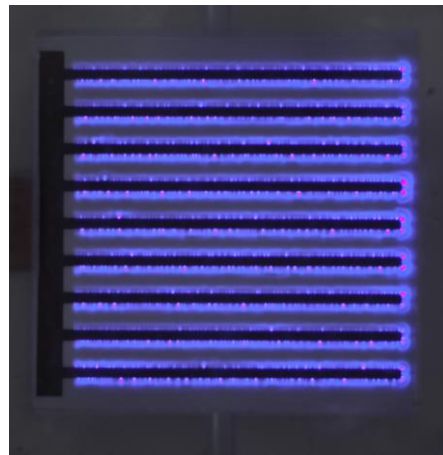
Fig. 16: Photograph of the discharge. Discharge voltage 3.12 kV.

The voltage was supplied by function/arbitrary waveform generator RIGOL DG1022 and amplified with wideband AC power amplifier. For the experiment, a sinusoidal waveform with frequency 10 kHz was utilized. The waveform generator RIGOL DG1022 has the following specifications:

- Amplitude range from 2 mV$_{p-p}$ to 10 V$_{p-p}$ for 50 Ω impedance and from 4 mV$_{p-p}$ to 20 V$_{p-p}$ for high impedance output.
- Amplitude accuracy ± 1% of setting + 1 mV$_{p-p}$
- Amplitude flatness 0.1 dB (for <100 kHz frequencies)
- Frequency range from 1 µHz to 20 MHz for a sinusoidal wave generation

The RIGOL DG1022 waveform generator is illustrated in Fig. 17.

For the measurement of the electrical parameters, the digital oscilloscope RIGOL DS1204B was utilized. For the measurement of discharge voltage, the high voltage probe Pintek HVP-28 was used, connected to the CH1 of the oscilloscope. Pearson Current Monitor 2877 was connected to CH2 and the voltage.
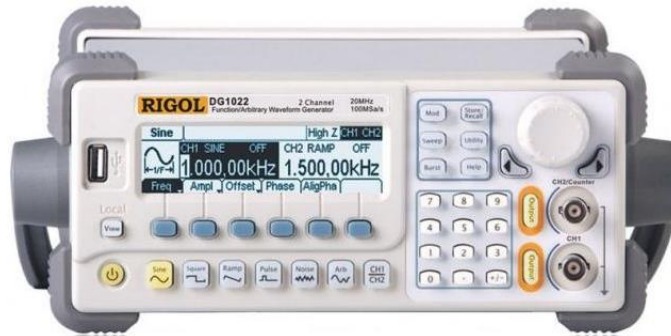

Fig. 17: RIGOL DG1022 waveform generator (source: www.toolboom.com)

The RIGOL DS1204B digital oscilloscope is illustrated in Fig. 18, the yellow curve corresponds to the discharge voltage, measured with the high voltage probe, the blue curve corresponds to the output of the current monitor.
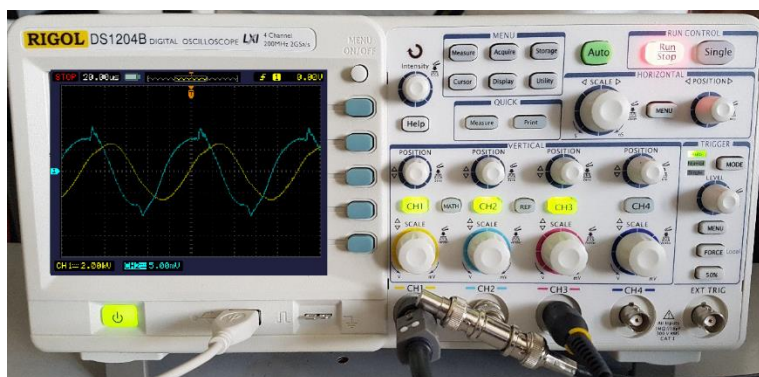

Fig. 18: RIGOL DS1204B Digital Oscilloscope

The RIGOL DS1204B has the following characteristics:

- Input impedance 1 MΩ± 2.0%

- Input capacitance 18 pF± 3pF

- Maximum input voltage 1000 V

- The typical time delay between channels 500 ps

- Bandwidth 200 MHz

- 8 Bit resolution and 2 GS/S sampling rate

To measure the concentration of the generated ozone the Ozone Analyzer BMT 964 was used. For measurement of NO_x concentration, MD Madur GA-60 Gas Analyzer was used.

The principle of measurement of the ozone concentration in the Ozone Analyzer BMT 964 is based on a previously mentioned property of ozone, being high absorbent of UF radiation on 254 nm wavelength. The analyzer utilizes an extremely long-life mercury lamp that emits radiation mostly at 254 nm wavelength. The generated ozone is supplied to the absorption cell via a plastic pipe. The sample in the cell is irradiated with the use of mercury lamp and the absorption is analyzed with photometer with true dual beam optical system. Then the cell is cleaned from ozone with air flow and the absorption is analyzed again and the whole cycle repeats.

The concentration of the ozone is calculated on the basis of the relation of absorption of light in case of ozone and air, being present in the absorption cell. The concentration is calculated with the Beer-Lambert-Bouguer law:

$$C_{O_3} = -\frac{T}{273\ K} * \frac{101.32\ kPa}{P} * \frac{10^9}{m*l} * \ln\left(\frac{L}{L_0}\right), \tag{26}$$

Where T is the temperature in Kelvins, P is the pressure in mercury lamp, m is the absorption coefficient, l is the absorption length, L is the light intensity, passing through a gas sample containing ozone and L_0 is the light intensity, passing through a gas sample after air cleaning of the chamber.

It is seen from equation (26) that the concentration of ozone also depends on the temperature and pressure that is why the analyzer is equipped with a thermometer and with built-in cuvette pressure transducer, for ozone measurement at an arbitrary systemic pressure.

The ozone analyzer is illustrated in Fig. 19:

Fig. 19: Ozone Analyzer BMT 964.

The device has the following characteristics:

- Measurement range from 1 ppm to 2500 ppm
- Zero drift 0.2% of range per day after the warm-up
- Temperature range (ambient) from 0 to 50 °C
- Recommended flow rate from 0.1 to 1 l/min
- Accuracy 0.4% of measurement + 0.1% of scale
- Response time 0.3 s (for display)
- 4-20 mA and 0-10 V isolated analog outputs
- Power supply 100-240 V AC, 15 VA
- Bidirectional RS-232 interface with baud rate up to 38400 for readout of event and error logs on a Windows PC

The data (voltage on 2 different channels and time) from the digital oscilloscope RIGOL DS1204B were copied as .csv and .bmp files to a flash drive for further analysis on PC.

5.1. Experimental Results.

The experiments were performed with the DBD in the air at atmospheric pressure and ambient temperature 24 °C. The concentration of ozone and nitric oxides was measured after the concentration reached the stable state. The results of the experiment are shown in the Tab. 4. The $V_{f.g.}$ is the voltage, supplied from the waveform generator.

Experiment Number	$V_{f.g.}$ (mV)	V_{max} (kV)	O_3 concentration (ppm)	NO_2 concentration (ppm)
1	280	2.16	34	7
2	300	2.24	120	40
3	320	2.32	202	96
4	340	2.40	274	149
5	360	2.56	321	178
6	380	2.72	371	212
7	400	2.88	410	235
8	420	2.96	462	262
9	440	3.12	512	294

Tab 4: Ozone and nitric dioxide concentration with different discharge voltages.

To study the ozone and nitric dioxide generation with DBD at atmospheric pressure and dry air utilization it is essential to calculate the average power, dissipated in the discharge for each of the configurations of the input voltage. It is important to find the dependence of the concentration of active species versus the average power and versus discharge voltage. To calculate the power, dissipated in the discharge the formula (8), applied to the function of voltage (measured with high voltage probe on Channel 1 of the oscilloscope) and function of current (measured with Pearson Current Monitor on Channel 2 on the oscilloscope) was used.

In the experiment, the frequency was 10 kHz. The digital data from oscilloscope was saved in .csv files on a flash drive and processed on PC with aid of Excel application. The Excel does not include functionality for numerical integration of functions the calculation of the integral was programmed manually. The trapezoid method of integration was implemented.

The results of the average power calculation are presented in the Tab. 5:

Experiment Number	$V_{f.g.}$ (mV)	V_{max} (kV)	Average power (W)
1	280	2.16	0.39
2	300	2.24	0.86
3	320	2.32	1.66
4	340	2.40	2.25
5	360	2.56	2.71
6	380	2.72	3.16
7	400	2.88	3.51
8	420	2.96	3.99
9	440	3.12	4.50

**Tab 5:** Average power, calculated for different input voltages.

As it is seen from the Tab. 5, the average power increases with the increase of discharge voltage. The dependence of the average power versus discharge voltage is illustrated in Fig. 20:
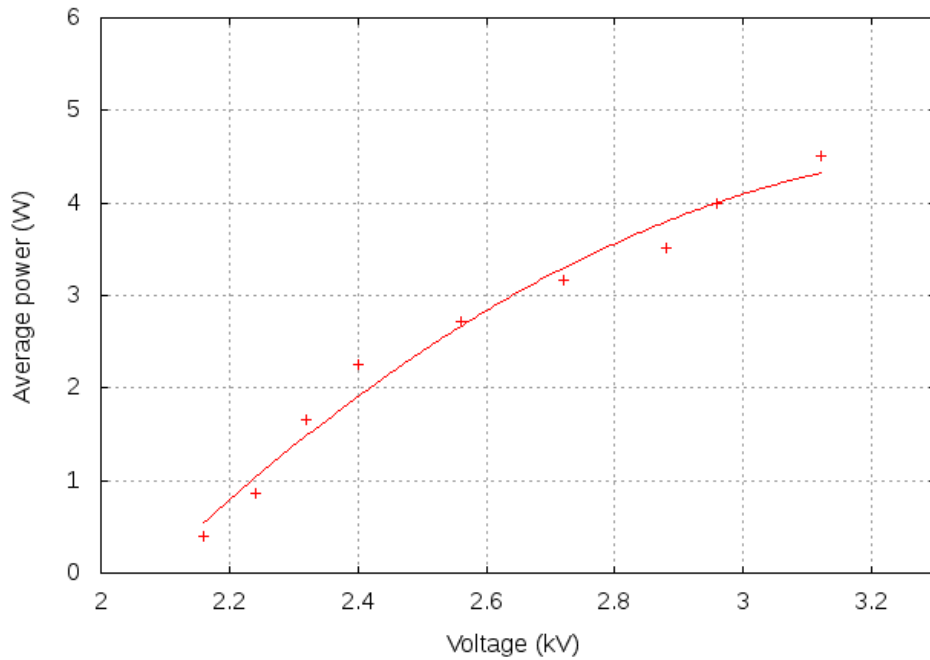
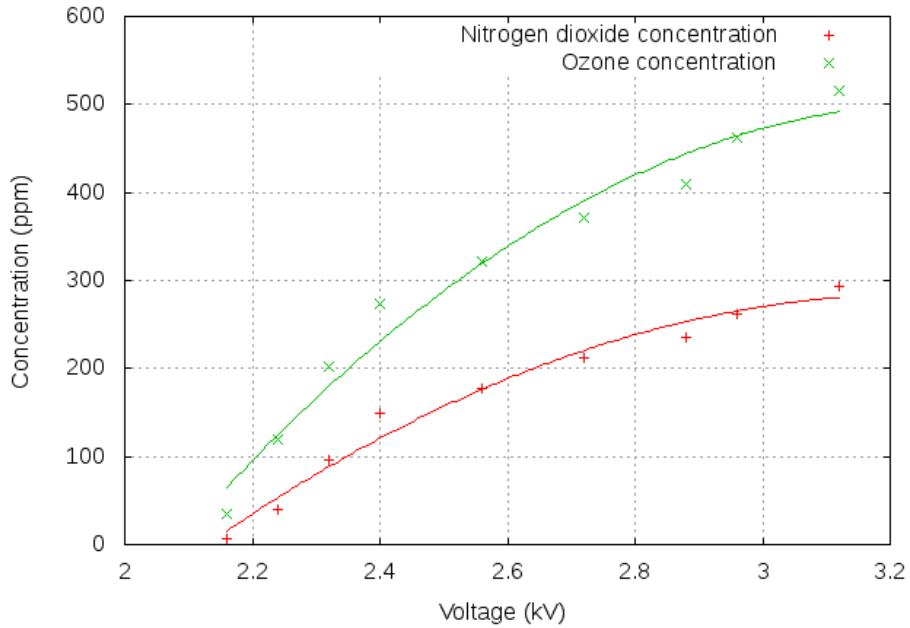**Fig. 20:** Average power versus discharge voltage.

From Fig.20 it is seen that average power increases with the increase of discharge voltage. In Fig. 21 the snapshots of both electrical signals, recorded on the oscilloscope, are presented.
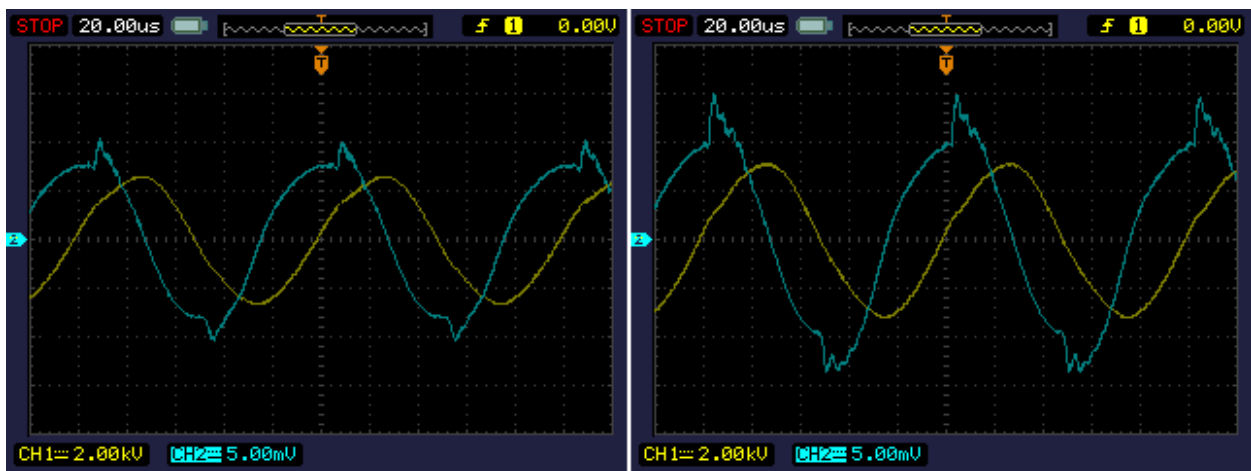
Fig. 21: Snapshot of both electric signals on the digital oscilloscope (yellow corresponds to discharge voltage, measured with high voltage probe; blue corresponds to current (1 V/A), measured with Pearson Current Monitor) (Left figure corresponds to the experiment №5, right snap corresponds to the experiment №9.

From Fig. 21 it is possible to conclude that the increase of average power depends on the microdischarge activity. This activity corresponds to the abrupt current pulses on the blue curve.

The purpose of this thesis was to study the ozone and nitric dioxide generation with DBD. To analyze this generation, it is necessary to investigate the dependence of the concentration of both active species versus discharge voltage. The dependence is presented in Fig. 22:

Fig. 22: Concentration of ozone and nitric dioxide versus discharge voltage.

For economical evaluation it is necessary to investigate the change of concentration of ozone and nitric dioxide with the change of power, as increasing power means increasing energy costs of generation, therefore dependence of the concentration of ozone and nitric dioxide versus the average power was analyzed. The dependence is presented in Fig. 23.

The dependence of the ozone concentration versus average power is linear up to 4.5 W with maximum non-linearity 11.5%. The dependence of the nitrogen dioxide concentration versus average power in linear up to 4.5 W with maximum non-linearity 3.9% (see Fig. 23). The concentration of both active species reaches their maximum at the maximum voltage (and power), in the case of experiment №9. This means that the increase of average power up to 4.5 W is economically feasible, as the concentration of active species increases almost linearly.
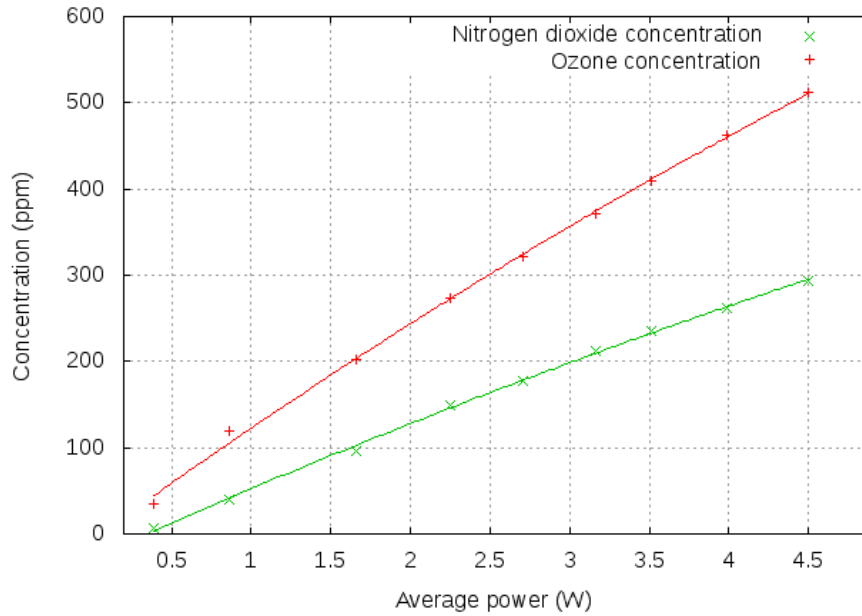
Fig. 23: Concentration of ozone and nitric dioxide versus average power.

6. Conclusions.

The presented bachelor thesis had four objectives:

1. To review the theory of non-thermal electrical discharges, utilized in processes of active species generation at atmospheric pressure.
2. To review the fundamental electrical parameters, describe the measuring apparatus and methods for analysis of those parameters.
3. To review the processes, connected with the ozone and nitrogen oxide generation and destruction.
4. To measure and analyze the concentration of ozone and nitrogen oxides with respect to the average power.

The two types of non-thermal electrical discharges, utilized in active species generation are dielectric barrier discharge and corona discharge. For the experimental part of this thesis, the dielectric barrier discharge was chosen, as it is possible to achieve a higher concentration of ozone. The concentration of ozone and nitrogen dioxide was analyzed as a function of discharge voltage and as a function of average power. The graph of the average power versus discharge voltage was presented.

From the analyzed data it is seen that the dependence of the concentration of ozone and nitrogen dioxide increases linearly with respect to power (for dissipated power up to 4.5 W).

In the experiment, the temperature increase due to the discharge was not enough to disturb the linearity. The impact of nitrogen dioxide was not sufficiently large to significantly reduce the ozone concentration. To keep the concentration of generated ozone high it is vital to provide low enough temperature to prevent the thermal destruction of ozone.

Ozone generation with dielectric barrier discharge is a promising method for industrial applications, the future investigation of properties and parameters of the discharge will lead to the increase of efficiency and decrease of cost of generated species.

7. Bibliography/ References.

[1] A Fridman, A Chirokov and A Gutsol, 2005, Non-thermal atmospheric pressure discharges. J. Phys. D: Appl. Phys. 38 (2005) R1-R24.

[2] M. A. Malik, Nitric Oxide Production by High Voltage Electrical Discharges for Medical Uses: A Review. Plasma Chem Plasma Process 36 (2016) 737-766.

[3] S. Pekarek, Experimental Study of Nitrogen Oxides and Ozone Generation by Corona-Like Dielectric Barrier Discharge with Airflow in a Magnetic Field. Plasma Chem Plasma Process (2017). DOI 10.1007/s11090-017-9831-9.

[4] J. Mikeš, S. Pekárek, and I. Soukup, Experimental and modelling study of the effect of airflow orientation with respect to strip electrode on ozone production of surface dielectric barrier discharge. Journal of Applied Physics, 120 (2016) 173301

[5] K.H. Becker, U. Kogelschatz, K.H. Schoenbach, R.J. Barker, 2004, Non-Equilibrium Air Plasmas at Atmospheric Pressure. Institute of Physics, Series in Plasma Physics, 2005, Bristol and Philadelphia

[6] I. A. Souza, A. B. Neto, , J. C. Queiroz, E. P . Matamoros, T. H. Costa, M. C. Feitor, . . . V.D. Sobrinho, (2016). Study of the Influence of Variation in Distances Between Electrodes in Spectral DBD Plasma Excitation. *Materials Research, 19*(1), 202-206. doi:10.1590/1980-5373-mr-2015-0205

[7] S. Zhang, C. Ping, Y. Tarasenko, V. Lomaev, M. Sorokin, D. Kozyrev, A. Baksht, (2012). Spark discharge formation in an inhomogeneous electric field under conditions of runaway electron generation. Journal of Applied Physics. 111. 10.1063/1.3677951.

[8] S. Pekarek, Asymmetric properties and ozone production of surface dielectric barrier discharge with different electrode configurations. The European Physical Journal D (2013). DOI 10.1140/epjd/e2013-30723-4.

[9] W. V. Siemens, Annalen der Chemie und Physik 102, 66 (1857).

[10] S. Pekárek, J. Rosenkranz, J. Khun. Ozone generation from two hollow needles to plate electrical discharges enhanced by an airflow. 12th International Congress on Plasma Physics, 25-29 October 2004, Nice (France). 2004. <hal-00001848v2>

[11] S. Tumanski, *Handbook of Magnetic Measurements*, CRC Press, 2011, ISBN 1-439-82952-7